論文

Electro-Micromechanical 시험법을 이용한 섬유 함침 각에 따른 탄소와 SiC 섬유강화 에폭시 복합재료의 계면 손상 감지능 및 평가

박종만*+, 이상일**, 공진우***, 김태욱***

Interfacial Damage Sensing and Evaluation of Carbon and SiC Fibers/Epoxy Composites with Fiber-Embedded Angle using Electro-Micromechanical Technique

Joung-Man Park*+, Sang-Il Lee**, Jin-Woo Kong***, Tae-Wook Kim***

ABSTRACT

Interfacial properties and electrical sensing for fiber fracture in carbon and SiC fibers/epoxy composites were investigated by the electrical resistance measurement and fragmentation test. As fiber-embedded angle increased, the interfacial shear strength (IFSS) of two-type fiber composites decreased, and the elapsed time takes long until the infinity in electrical resistivity. The initial slope of electrical resistivity increased rapidly to the infinity at higher angle, whereas electrical resistivity increased gradually at small angle. Furthermore, both fiber composites with small embedded angle showed a fully-developed stress whitening pattern, whereas both composites with higher embedded angle exhibited a less developed stress whitening pattern. As embedded angle decreased, the gap between the fragments increased and the debonded length was wider for both fiber composites. Electro-micromechanical technique could be a feasible nondestructive evaluation to measure interfacial sensing properties depending on the fiber-embedded angle in conductive fiber reinforced composites.

초 록

Fragmentation 시험법과 전기저항 측정을 통하여 탄소 및 SiC 섬유강화 에폭시 복합재료의 계면물성과 섬유파단에 대한 전기적 감지능을 연구하였다. 섬유 함침 각이 증가함에 따라서 계면전단강도는 감소하였고, 섬유파단에 의한 전기저항도 값이 무한대로 증가하는 시간은 길어졌다. 높은 함침 각에서 전기저항도의 초기 기울기는 급격히 증가한 반면, 낮은 각에서는 점차적으로 증가하였다. 또한 낮은 함침각의 두 섬유 모두에서 stress whitening pattern을 뚜렷하게 관찰할 수 있었지만, 높은 함침 각에서는 그렇지 못했다. 섬유 함침 각이 감소함에 따라서 섬유 파단 간격과 debonding된 길이는 두 섬유 모두에서 증가하였다. 본 연구에서 사용한 electro-micromechanical 시험법은 전도성 섬유강화 복합재료의 섬유 함침 각에 따른 계면 감지능 측정을 위해서 비파괴적 평가방법으로 실행 가능하였다.

Key Words: 전기적 손상감지능(Electrical damage sensing), 비파괴시험(Nondestructive test), 음향방출(Acoustic emission), 계면전단강도(Interfacial shear strength (IFSS)), 응력전달(Stress transfer)

*+ 경상대학교 응용화학공학부 고분자공학전공, 공학연구원, 교신저자 (E-mail: jmpark@nongae.gsnu.ac.kr)

** University of Nebrasca-Lincoln, U.S.A.

*** 한국기계연구원 복합재료그룹

1. Introduction

Using the electrical resistivity measurement, a new evaluation technique of interfacial properties as well as curing characteristics and the residual stress were investigated recently in various conductive fiber reinforced composites[1]. The electro-micromechanical technique had been studied as economically a new nondestructive evaluation (NDE) method for monitoring of curing characteristics, interfacial properties and nondestructive behavior because conductive fiber can act as a sensor in itself as well as a reinforcing fiber[2,3]. Yuse *et al.*[4] used the electrical resistance measurement as one of the intelligent nondestructive testing (NDT) method. The relationship between electrical resistance and fiber breakage/delamination in carbon fiber reinforced plastic (CFRP) laminate was studied under tensile and fatigue tests.

AE is well known as one of the important NDT methods. AE can monitor the fracture behavior of composite materials, and can characterize many AE parameters to understand the type of microfailure sources during the fracture progressing. When tensile loading is applied to a composite, AE signal can occur from fiber fracture, matrix cracking, and possibly debonding at the fiber-matrix interface. AE energy released by the fiber fracture could be greater than that associated by debonding or matrix cracking[5]. Park *et al.*[6] studied the micromechanical properties and microfailure mechanism of single-carbon fiber composites using AE and fragmentation test.

In this work, under tensile test, the measurement of electrical resistance and the analysis of AE signals in fiber/epoxy composite were used to evaluate interfacial properties and nondestructive behaviors depending on the different fiber-embedded angles. The relationship among the electrical resistivity, AE signal and IFSS were investigated for single fiber/epoxy composites.

2. Experimental

2.1 Materials

Carbon fiber of 8 ㎛ (Taekwang Industrial Co., Korea) in average diameter and SiC fiber (Ube Industrial Co., Japan) of 13 ㎛ were used as conductive reinforcing materials. Epoxy resin (Kukdo Chemical Co. YD-128, Korea) is based on diglycidyl ether of bisphenol-A (DGEBA). Polyoxypropylene diamines (Jeffamine D400 and D2000, Huntzman Pertochemical Co.) were used as curing agents. The flexibility of specimens was controlled by the mixing ratio of D400 *versus* D2000.

2.2. Methodologies

2.2.1 Preparation of Testing Specimens

The typical specimens were used for fragmentation test, curing monitoring and electro-micromechanical test. Fig. 1(a) exhibits a testing specimen to evaluate electrical resistivity as a function of various embedded angles by the electro-micromechanical testing. Fig. 1(b) shows dogbone-type specimen that is single carbon fiber composites to measure IFSS and AE signals.

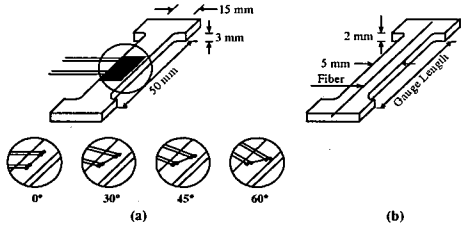

Fig. 1 Test specimens of single fiber composites for (a) electrical resistivity and (b) IFSS and AE signal.

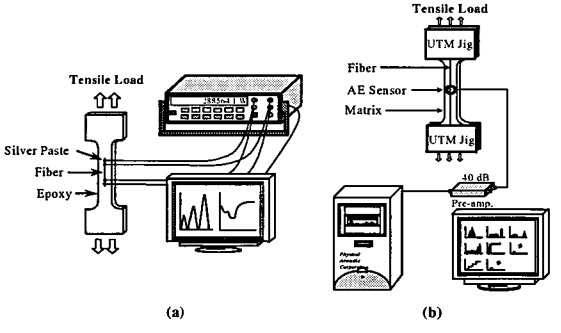

Fig. 2 Experimental system for (a) electrical resistivity measurement and (b) acoustic emission.

2.2.2 Electrical Resistance Measurements

The electrical resistance was measured using a digital multimeter (HP34401A). For the electrical resistance measurement under tensile load, the stress-strain curve was measured by universal testing machine (UTM, Lloyd Instruments Co., U.K.). Fig. 2(a) shows the experimental scheme showing the measurement of electrical resistance and stress-strain curve in single fiber composite. Electrical resistivity was obtained from the measured electrical resistance, cross-sectional area of the conductive fiber, A, and

Table 1 Intrinsically electrical properties of two conductive fibers

Fiber	Diameter (μm)	Electrical Resistance (Ω)	Electrical Resistivity ($\Omega \cdot cm$)=10^{-3}
Carbon[1)]	8	$1.19=10^4$	1.86
Carbon[2)]	18	$1.57=10^3$	1.25
SiC[3)]	10	$8.79=10^5$	215.7
SiC[3)]	13	$8.36=10^5$	346.6

1) PAN-based (Taekwang Industrial Co., Korea)
2) Pitch-based (Mitsubishi Chemical Co., Japan)
3) Silicon Carbide-based fiber (Ube Industrial Co., Japan)

$$\rho = \frac{L_{ec}}{A} \times R \quad (1)$$

electrical contact length, L_{ec} of the testing fiber connecting to copper wire. The relationship between electrical resistivity, ρ and resistance, R is as follows:

2.2.3 IFSS Measurement and AE Test

To evaluate IFSS and AE signals depending on the embedded angle, UTM was used with a polarized-light microscope and AE system. The specimens were tested by UTM (Load cell of 10 kN, cross-head speed of 0.5 mm/sec.) while AE monitoring. After the testing specimen was fixed in the tensile testing machine, the composite was strained incrementally and the fiber was broken into small fragments embedded in the matrix until no longer fiber fracture occurred.

IFSS was determined by Drzal equation[7] that was modified from Kelly-Tyson equation[8]. By introducing the Weibull distribution for the aspect ratio, IFSS was exhibited in the form as follows:

$$\tau = \frac{\sigma_f}{2 \cdot \alpha} \cdot \Gamma[1-1/\beta] \quad (2)$$

where α and β are scale and shape parameters of Weibull distribution for aspect ratio (l_c/d), and is the gamma function.

AE signals were detected using a miniature sensor (Resonance Type, PICO by PAC Co.) with peak sensitivity of 54 Ref V(m/s) and resonant frequency at 500 kHz. The sensor output was amplified by 40 dB at preamplifier gain. The threshold level was set up as 30 dB. The signal was fed into an AE signal process unit (MISTRAS 2001), where AE

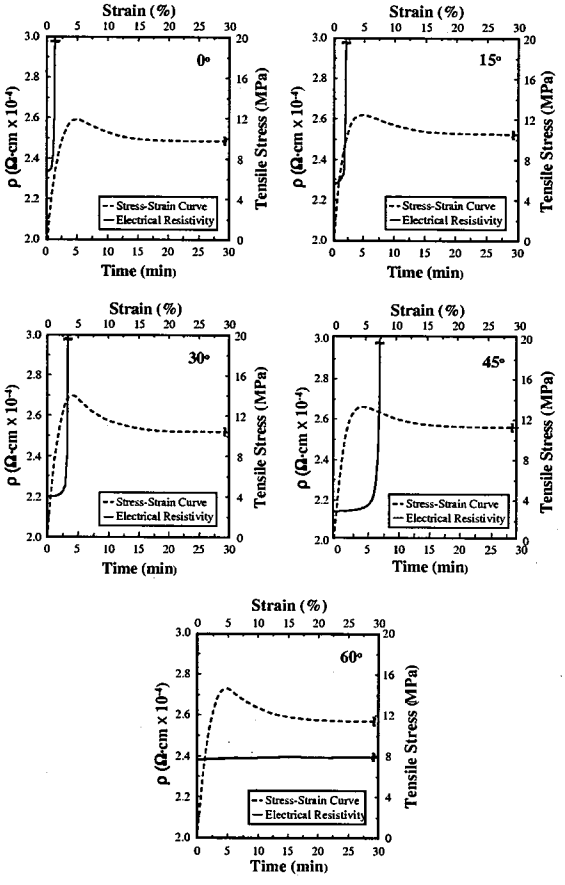

Fig. 3 Electrical resistivity and stress-strain curve for carbon fiber composites.

parameters were analyzed using an in-built software. The typical AE parameters such as hit rate, peak amplitude, and event duration were investigated for the time and the distribution analysis. Fig. 2(b) shows schematic AE diagram.

3. Results and Discussion

3.1 Electrical Properties of Two Conductive Fiber

Table 1 shows intrinsically electrical properties of two conductive fibers. Electrical resistance was measured by four-point probe method. Silver paste was used as electrically connecting glue at junctions to maintain an electrical contact between the fiber and leading wire.

Fig. 3, 4 show electrical resistivity and stress-strain curve

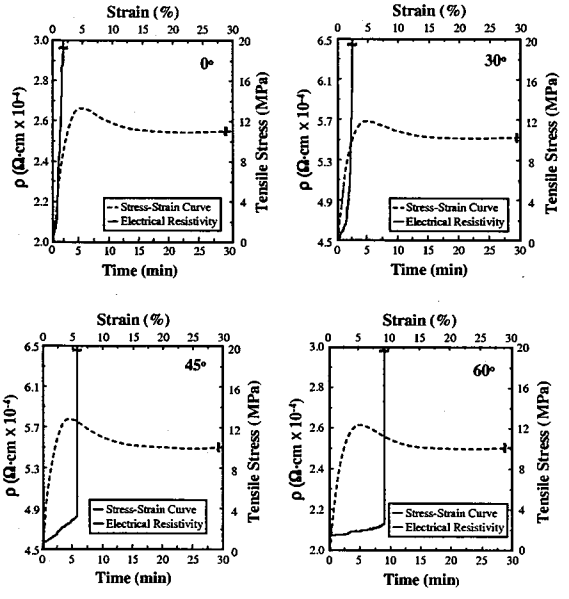

Fig. 4 Electrical resistivity and stress-strain curve for SiC fiber composites.

Table 2 Interfacial properties of carbon and SiC fiber composites

Embedded Angle (Degree)	Carbon Fiber						Carbon Fiber		
	Critical Fragment Length (μm)	Aspect Ratio (l_c/d)	α[1]	β[2]	IFSS Kelly	IFSS Drzal	Critical Fragment Length (μm)	Aspect Ratio (l_c/d)	IFSS[3] (MPa)
0	533.5	66.7	72.2	5.43	37.1	35.0	871	67	35.1
15	614.3	76.8	83.1	5.50	31.3	29.6	-	-	-
30	757.1	94.6	102.2	5.61	24.4	23.2	1162	89	25.5
45	888.9	111.1	120.5	5.20	20.4	19.1	1477	114	19.3
60	-	-	-	-	-	-	1747	134	16.0

1) Scale parameter
2) Shape parameter
3) Calculated from Kelly-Tyson Eq.

in single carbon and SiC fiber/epoxy composites. As the fiber-embedded angle increased, elapsed time to the infinity in electrical resistivity increased and the initial slope of electrical resistivity also gradually increased.

3.2 Interfacial Properties of Single Fiber/Epoxy Composites

Table 2 shows interfacial properties and statistical Weiblull parameters of single carbon and SiC fiber/ epoxy composites with fiber-embedded angles. As the fiber embedded angle increased, the average fragment length and aspect ratio, l_c/d,

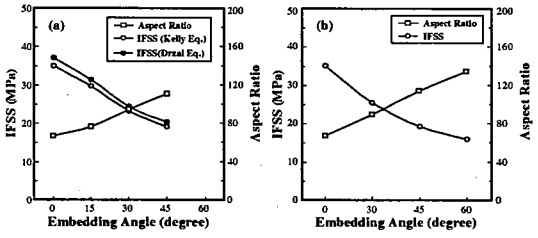

Fig. 5 IFSS and aspect ratio depending on fiber-embedded angle.

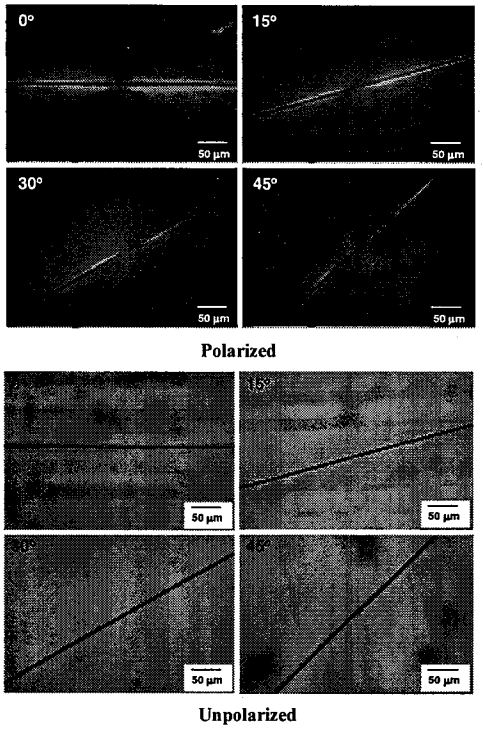

Fig. 6 Initial fiber failure modes and stress whitening for carbon fiber composites.

were larger and IFSS decreased. Fig. 5 shows IFSS and aspect ratio depending on fiber-embedded angles. In case of single carbon fiber/epoxy composite, IFSS for 60 degree was not measured, because the fiber for 60 degree was not broken.

3.3 Microfailure Modes

Fig. 6 shows the comparison of fully developed whitening and initial fiber failure modes of carbon fiber/epoxy composites. As the fiber-embedded angle increased, the fully developed stress birefringence pattern was smaller. Strains of

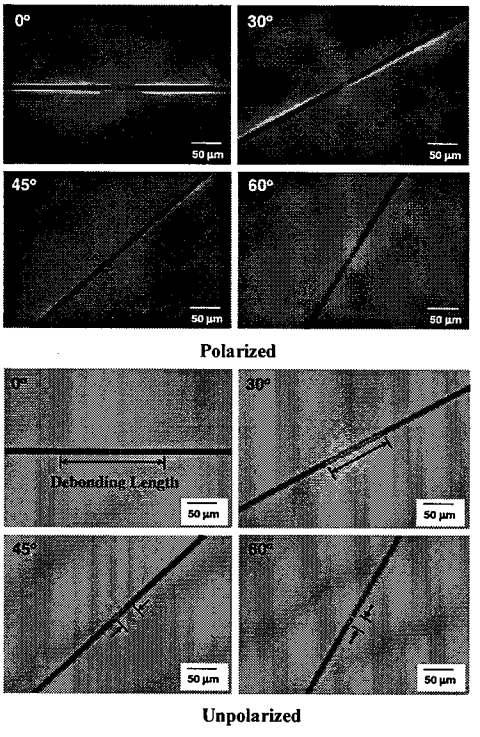

Fig. 7 Initial stress whitening and final debonding length for SiC fiber composites.

first fiber breakage are 1.18 % for 0 degree, 2.7 % for 15 degree, 4.0 % for 30 degree and 7.8% for 45 degree, respectively. The fiber for 60 degree was not broken. The first fiber breakage occurred late as the fiber-embedded angle increased. As shown in Fig. 6 and 7, when the fiber was broken, the crack shape of matrix was not cone shape. Because the transferring load to matrix was very small, the matrix crack was not shown. Fig. 7 shows initial and final microfailure modes of SiC fiber/epoxy composites. As the fiber-embedded angle decreased, the gap between fragments increased.

3.4 AE Outcomes

Fig. 8, 9 show results of AE energy and AE amplitude, and Fig. 10 shows AE waveforms of single carbon fiber composite. AE energy and AE amplitude for small angle case were higher than high angle case and the main signal group appeared late in the elapsed time. As the fiber-embedded angle increased, the fiber signals were reduced and the voltage of AE waveform decreased more. This might be due to the difference in microfailure mechanisms depending on

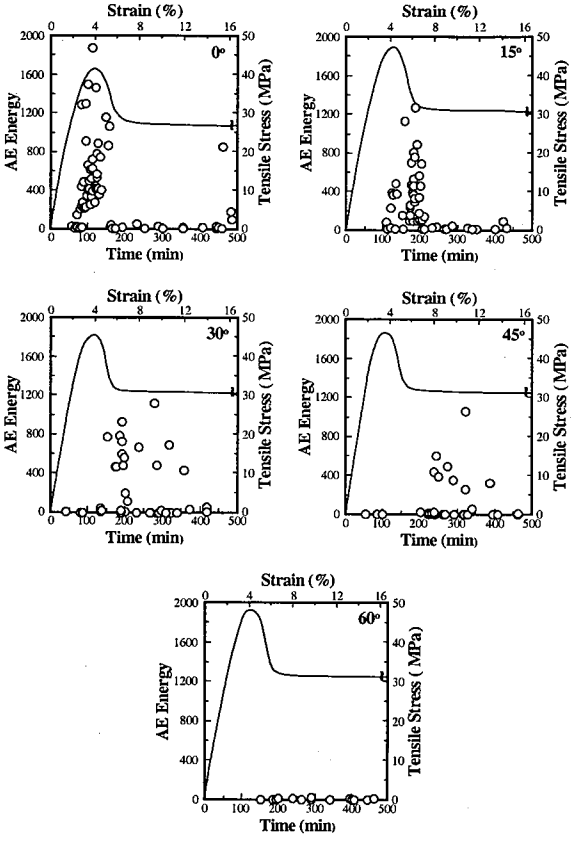

Fig. 8 AE energy and stress-strain curve depending on fiber-embedded angle.

fiber-embedded angles. In carbon fiber composite, fiber fracture was not occurred in 60 degree case.

4. Conclusions

Electrical resistance of carbon and SiC fiber composites was responded well during the measurement of interfacial sensing properties. As the fiber-embedded angle increased, the elapsed time to the infinity for electrical resistivity increased. As fiber-embedded angle decreased, IFSS increased and the elapsed time was faster to infinity at the first fiber fracture in both two fibers. The specimen with small angle showed fully developed stress whitening patterns, whereas that the case with higher angle showed less developed stress whitening pattern. AE events were detected well under tensile load. As the fiber-embedded angle increased, AE energy was gradually smaller and main signal groups appeared late in the

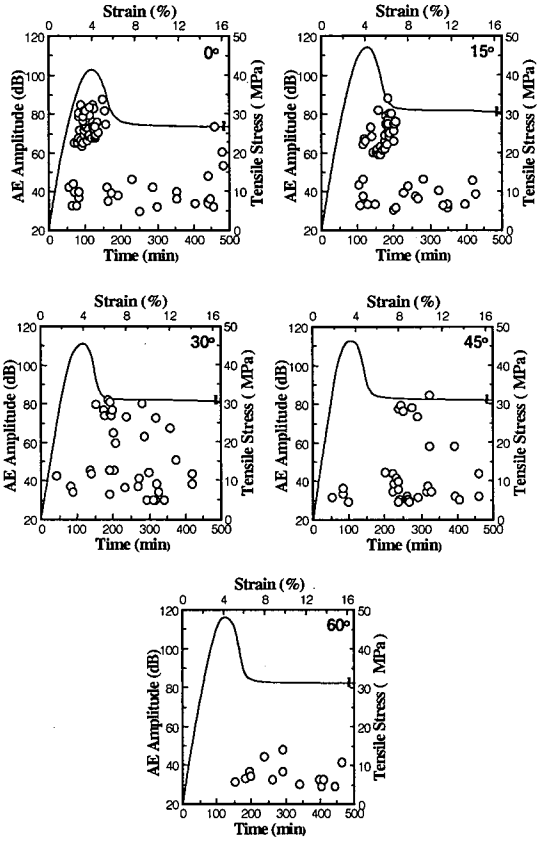

Fig. 9 AE amplitude and stress-strain curve depending on fiber-embedded angle.

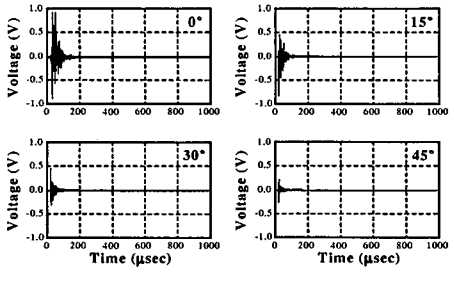

Fig. 10 AE waveforms of single carbon fiber composite.

elapsed time. AE voltage of the waveform of carbon fiber breaks for the small angle exhibited much larger than that for higher angle.

Acknowledgment

This work was financially supported from CNMT of the 21st C Frontier R&D program (NM02-1201-001-1-0-2) by Ministry of Science and Technology (MST), through Engineering Research Institute (ERI), GNU.

References

1) D. M. Bontea, D. D. L. Chung and G. C. Lee, "Damage in carbon fiber-reinforced concrete monitored by electrical resistance measurement," *Cement and Concrete Research*, Vol. 30, 2000, pp. 651-659.

2) X. Wang and D. D. L. Chung, "Residual stress in carbon fiber embedded in epoxy, studied by simultaneous measurement of applied stress and electrical resistance," *Composites Interface*, Vol. 5, 1998, pp. 277-281.

3) X. Wang and D. D. L. Chung, "An electromechanical study of the transverse behavior of carbon fiber polymer-matrix composites," *Composites Interface*, Vol. 5, 1998, pp. 191-199.

4) K. Yuse and C. Bathias, "Smart NDT using electrical resistance method for delamination monitoring in CFRP," *In Proceeding ICCM-12*. Paris, France, 1999, pp. 767-776.

5) J. M., Park, W. G. Shin and D. J. Yoon, "A study of interfacial aspects of dual basalt and SiC fibers reinforced epoxy-based composites by means of the fragmentation and acoustic emission techniques," *Composites Science and Technology*, Vol. 59, 1999, pp. 355-370.

6) J. M., Park, E. M. Chong, D. J. Yoon and J. H. Lee, "Interfacial properties of two SiC fiber-reinforced polycarbonate composites using the fragmentation test and acoustic emission," *Polymer Composites*, Vol. 11, 1998, pp. 747-758.

7) L. T. Drazal, "The effect of polymeric matrix mechanical properties on the fiber-matrix interfacial shear strength," *Material Science and Engineering*, Vol. 21, 1990, p. 289-293.

8) A. Kelly and W. R. Tyson, "Tensile properties of fiber reinforced metals: copper/tungsten and copper/molybdenum," *Journal of Mechanical and Physis Solids*, Vol. 13, 1965, pp. 329-350.